Available online at www.sciencedirect.com
SCIENCE DIRECT®
ELSEVIER
Journal of Magnetism and Magnetic Materials 293 (2005) 731–736
Journal of magnetism and magnetic materials
www.elsevier.com/locate/jmmm

Towards a magnetic microarray for sensitive diagnostics

Shan X. Wang[a,b,*], Seung-Young Bae[a], Guanxiong Li[a], Shouheng Sun[c], Robert L. White[a,b], Jennifer T. Kemp[d], Chris D. Webb[d]

[a]*Geballe Laboratory for Advanced Materials, Department of Materials Science and Engineering, Stanford University, McCullough Building Room 351, 476 Lomita Mall, Stanford, CA 94305-4045, USA*
[b]*Department of Electrical Engineering, Stanford University, Stanford, CA 94305-4045, USA*
[c]*IBM T. J. Watson Research Center, Yorktown Heights, NY 10598, USA*
[d]*Stanford Genome Technology Center, 855 California Av., Palo Alto, CA 94304, USA*

Available online 14 March 2005

Abstract

We present proof-of-concept experiments and modeling towards a high-sensitivity magnetic microarray which "tags" a DNA fragment (or other biological samples) with a high-moment magnetic nanoparticle (NanoTag), which is in turn detected by a high-sensitivity spin valve (SV) or magnetic tunnel junction (MTJ) detector array. The detector can count the number of magnetic tags with a resolution of 1–20 magnetic NanoTags, potentially counting individual biomolecules.

Keywords: Magnetic microarray; MagArray; NanoTag; Nanoparticles; Spin valve; Magnetic tunnel junction; Biodetection; DNA detection

A high-sensitivity quantitative DNA fragment (and protein) detection and identification system will open many new applications in the field of functional genomics and molecular diagnostics. It can also form the basis for a rapid response system to identify suspected pathogenic agents such as anthrax. The ideal detection system should be sensitive, rapid, portable, and inexpensive, preferably not requiring DNA amplification processes such as polymerase chain reaction (PCR). More specifically, the system should have the following characteristics: (1) one DNA fragment per tag, (2) each tag individually detectable, (3) a very large number of detectors per chip and (4) known efficiency of the attachment processes involved. We are developing a magnetic microarray (MagArray^{TM}) to achieve or closely approach the above requirements.

MagArray^{TM} uses custom-made monodisperse single-domain high-moment magnetic nanoparticles

*Corresponding author. Geballe Laboratory for Advanced Materials, McCullough Building, Room 351, 476 Lomita Mall, Stanford University, Stanford, CA 94305-4045, USA. Tel.: +1 650 723 8671; fax: +1 650 736 1984.
E-mail address: sxwang@ee.stanford.edu (S.X. Wang).

0304-8853/$ - see front matter © 2005 Elsevier B.V. All rights reserved.
doi:10.1016/j.jmmm.2005.02.054

(called NanoTags hereafter), with a mean diameter of approximately 100–1000 Å, as the tags. Since the tag dimensions are comparable to those of the target DNA fragment, and because of the attachment sequence, we expect perhaps one or at most two or three fragments per tag (desideratum #1). Our detector may detect a single NanoTag, so approaches satisfaction of desideratum #2. Since our spin valve (SV) or magnetic tunnel junction (MTJ) detectors are down to submicron in size, a detector density on the order of 10^6 detector/cm^2 can be realized, satisfying desideratum #3. A proper calibration process will achieve desideratum #4.

All current microarray systems utilizing fluorescent labeling (tagging) are inherently of low sensitivity because they require approximately 10^4 molecules to achieve a useful signal-to-noise ratio and are marginally quantitative because of the optical systems involved, of crosstalk and of bleaching [1]. The optical detection systems are usually used in conjunction with PCR.

A group at the Naval Research laboratory and NVE Corporation has demonstrated a conceptually similar magnetic detection system which they called BARC [2–5]. Their detector employed a giant magnetoresistive multilayer stack that is much less sensitive than a properly designed SV or MTJ detector described here. A group in Portugal has deployed SV sensors coupled with coils at proximity [6], and another group in Germany demonstrated that GMR multilayer biodetection was superior to fluorescent biodetection [7]. The commercially available magnetic tags used by these groups tend to have a mean diameter in the range from 0.3 to 3 μm, including the paramagnetic polystyrene beads and similarly sized ferromagnetic particles. The larger tags will be coupled to a much larger and not easily ascertainable number of DNA fragments, prejudicing the quantitative capabilities of the system.

The combination of SV and MTJ sensor arrays and magnetic NanoTags constitutes a promising architecture for a sensitive, quantitative, non-optical detection system for DNA microarrays, a universal platform for many different biological assays. The basic methodology of such a magnetic microarray is shown in Fig. 1: (a) SV or MTJ sensor array is fabricated by optical or e-beam lithography, then bound with known DNA probes, (b) unknown DNA fragments (called targets) are labeled by high-moment magnetic NanoTags and (c) tagged DNA fragments are selectively captured by complementary DNA probes, and the magnetic NanoTags are read out by SV or MTJ sensors.

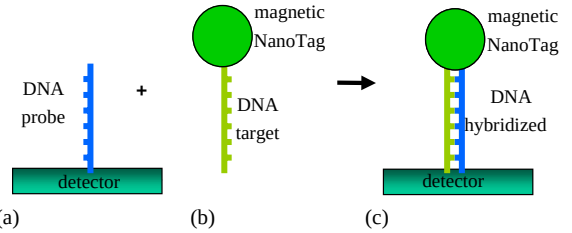

Fig. 1. Principle of a magnetic microarray based on magnetic NanoTags and spin valve or MTJ detectors.

As a proof of the above concepts, micro-sized and submicron-sized SV sensor arrays were fabricated by photolithography and e-beam lithography with the following layers: Si/Ta 3 nm/Seed layer 4 nm/PtMn 15 nm/$Co_{90}Fe_{10}$ 2 nm/Ru 0.85 nm/$Co_{90}Fe_{10}$ 2 nm/Cu 2.3 nm/$Co_{90}Fe_{10}$ 2 nm/Cu 1 nm/Ta 4 nm. These arrays have been successfully tested with a single micon-sized Dynabead® [8,9], 11-nm diameter Co NanoTags [8], and16-nm diameter magnetite (Fe_3O_4) NanoTags [10].

The detection scheme of SV sensor is illustrated in Fig. 2a. The pinned magnetic moment M_P of the SV sensor was fixed in the $-y$ direction and the free layer moment M_F rotated in response to an applied magnetic field H_a which was swept in the y direction (in-plane detection mode). Meanwhile, the resistance R of the SV sensor was measured using a four-probe method with the current-in-plane (CIP) configuration. The magnetoresistance (MR) transfer curves (R vs. H_a) were measured at room temperature before and immediately after magnetic NanoTags were coated onto the sensor. During the whole detection procedure, the experimental setup including the sensor chip remained untouched to ensure the identical configuration for MR transfer curve measurements. Therefore, the magnetic effect of the deposited NanoTags on the SV sensor was solely responsible for the difference

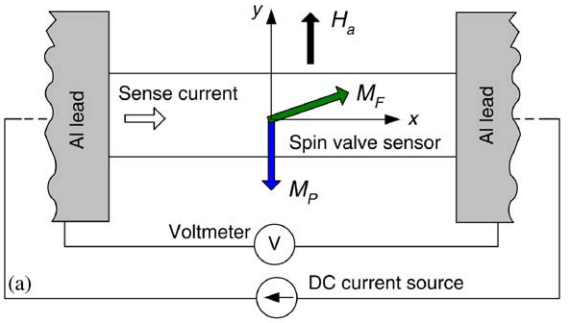

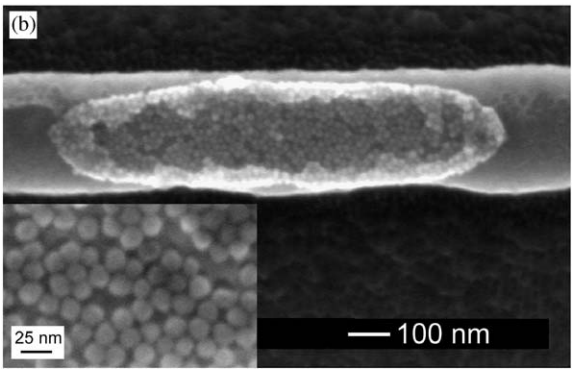

Fig. 2. Magnetic NanoTag detection. (a) The schematic drawing (top view) of the detection experiment. Using a four-probe method, two MR transfer curves of a SV sensor are measured before and after magnetic NanoTags are deposited, respectively. Comparing the two curves gives the net signal of the magnetic NanoTags. (b) SEM image of 16-nm Fe_3O_4 NanoTags deposited on a SV sensor on which the detection experiment was performed. The insert shows a part of the self-assembled NanoTags on the sensor at a higher magnification.

in the MR transfer curves taken with and without the NanoTags. The resistance differences obtained from the two curves were the net signal of the SV sensor due to the NanoTags.

Here, we demonstrate the quantitative detection of a patterned monolayer of 16-nm Fe_3O_4 NanoTags coated on 0.3-μm-wide SV sensors. A finite number (ranging from tens to hundreds) of monodisperse Fe_3O_4 [11] NanoTags were placed near the center of the SV sensor surface using a polyethylenimine-mediated patterned self-assembly method which will be published elsewhere [12]. Fig. 2b shows the 16-nm Fe_3O_4 NanoTags assembly on a SV sensor, which we used for the detection experiment and is referred as the "detection sensor" hereafter.

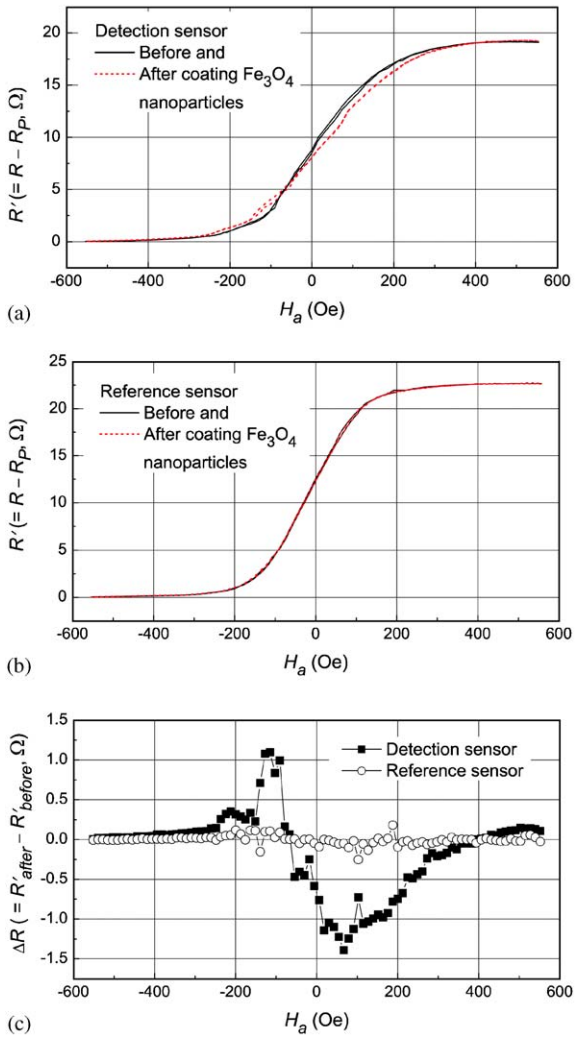

Fig. 3. MR transfer curves and resistance differences. The MR transfer curves (R' vs. H_a) measured before and after coating 16-nm Fe_3O_4 NanoTags for a SV detection sensor (a) and a reference sensor (b). (c) The resistance differences for the detection and reference sensors, respectively.

Fig. 3a shows the MR transfer curves measured on the detection sensor before and after coating with the Fe_3O_4 NanoTags. The relative resistance, $R' = R - R_P$, where R_P is the lowest base resistance of the SV sensor at parallel magnetization configuration, is plotted vs. the applied field H_a in the transfer curves to remove any spurious base resistance change not due to the MR effect such as

slight lead resistance variation. Apparent resistance differences are seen between the two MR transfer curves in Fig. 3a and are plotted in Fig. 3c as $\Delta R = R'_{\text{after}} - R'_{\text{before}}$, where R'_{before} and R'_{after} are the relative resistances before and after coating with NanoTags, respectively. To further confirm the effect of the NanoTags, we compared the MR transfer curves measured on a reference SV sensor during the same experiment. The reference sensor was on the same chip but was not coated with NanoTags. Fig. 3b shows the MR transfer curves from the reference sensor before and after Fe_3O_4 NanoTags were introduced on the detection sensor. The resistance differences of the reference sensor are also plotted in Fig. 3c. The essentially identical MR transfer curves of the reference sensor indicate that the resistance changes in the detection sensor are indeed caused by the Fe_3O_4 NanoTags.

Fig. 3c further indicates that the peak-to-peak resistance difference is about 2.3 Ω for approximate 630 Fe_3O_4 NanoTags shown in Fig. 2b. Therefore, the signal per NanoTag is roughly 3.7 mΩ, corresponding to a voltage of 3.7 μV if the sense current is 1 mA. If we take the standard deviation of the peak-to-peak resistance differences of the reference sensor as the detection limit, which is 72.4 mΩ, the minimum detectable number of the Fe_3O_4 NanoTags in this experiment is around 20 (at a signal-to-noise voltage ratio of ~1). An even lower detection limit may be reached in the future by using higher moment NanoTags (such as Co, Fe and CoFe), more sensitive sensors (such as MTJ to be discussed below), and lock-in detection.

The structure and detection scheme of MTJ biosensors are very similar to those of SV except that the Cu spacer is replaced with a tunnel barrier (typically aluminum oxide) and the sense current flows perpendicular to the plane (CPP). There are a number of advantages for MTJs over SV sensors. First of all, the magnetoresistance ratio (MR) of an MTJ is five times larger than that of SV. Higher junction resistances (typically several kiloohms and tunable by the tunnel barrier thickness) than SV resistances (~100 Ω for submicron-sized SV sensors) lead to much higher output voltages for a given number NanoTags. We present here our MTJ biosensor design and its preliminary performance.

MTJ biosensors were deposited by a magnetron sputter system with a layer stack of Si/500 Å Ta/500 Å Cu/50 Å Ta/18 Å CoFe/7 Å Ru/24 Å CoFe/Al-O/20 Å CoFe/50 Å Ta and were patterned by photolithography to a junction size of $1 \times 10\,\mu m^2$. Two step annealing of the junctions was performed: the first one for establishing the pinning field, and the second one for resetting the free layer orthogonal to the pinned layer. The total anisotropy field ($H_{k,\text{total}}$) of the free layer that determines the field sensitivity is ~50 Oe, which is the sum of the shape anisotropy (H_d) of ~20 Oe and the induced anisotropy (H_k) of ~30 Oe. When applying an external magnetic field along the hard axis of the free layer (i.e., along the easy axis of pinned layer), a tunneling magnetoresistance (TMR) ratio of ~50% was obtained at a low bias of 1 mV. There are two main mechanisms that set the upper limit of the applicable bias in MTJs. The first one is the breakdown of the dielectric tunnel barrier, which usually occurs at 1–2 V. The second and more relevant one is the bias dependence of TMR that exists in all MTJs. Fig. 4 shows that the TMR gradually drops with the increasing bias due to hot electron tunneling and magnon excitation at magnetic electrodes. The voltage signal ΔV can be calculated from the bias dependence of the TMR and is also shown in Fig. 4. The maximum ΔV

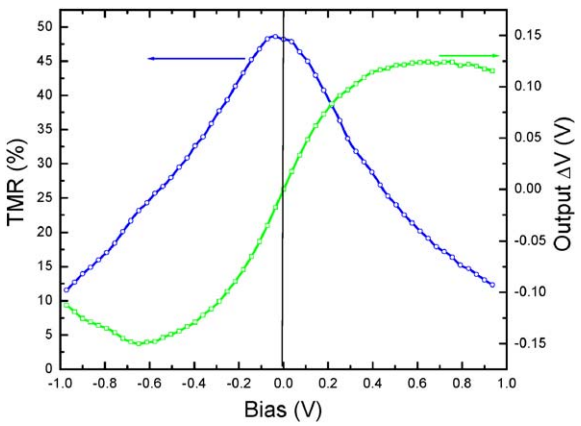

Fig. 4. The bias dependence of TMR (left y-axis) and output (ΔV, right y-axis) of a MTJ biosensor.

occurs in the bias range of 300–800 mV, largely independent of the junction size.

The usual MTJs are finished with thick (>100 nm) top electrodes. The top electrodes should be thick enough so that the electrode resistances are orders of magnitude smaller than junction resistances. Otherwise, the MTJs would suffer from reduced TMR due to the current crowding [13] within the top electrode area that overlaps the junction. Thick top electrodes increase the distance between the magnetic NanoTags and the free sensing layer in MTJs, degrading the signal per NanoTag since the magnetic field from a NanoTag decays with the distance between the Nanotag and the free layer. To address this issue, we designed a MTJ biosensor comprising of dual top electrodes as shown in the inset of Fig. 5. The first top electrode is a thin Au layer and the second top electrode is a thick Al layer with an opening to the underlying Au layer on the top of the active sensor area. In addition to minimizing current crowding, the Au surface facilitates specific DNA binding via gold-thiol linkage. Shown in Fig. 5 is the calculated TMR as a function of Au electrode thickness for $1 \times 10\,\mu m^2$ junction with RA (junction resistance × area) of $5\,k\Omega\,\mu m^2$. The reduction of TMR is less than 3% if the Au electrode is 5-nm thick.

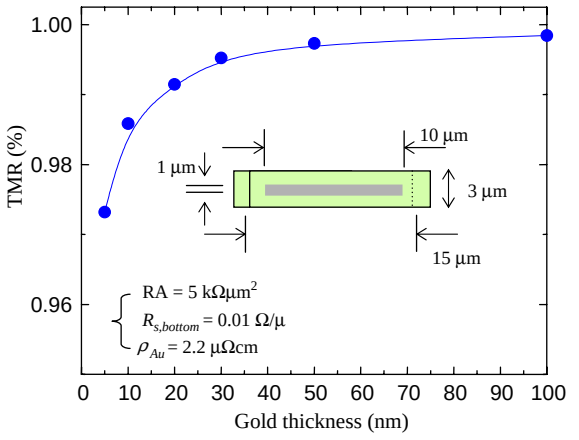

Fig. 5. Calculated TMR of a MTJ biosensor with dual top electrodes (inset) as a function of Au electrode thickness. The calculation was performed with FlexPDE finite element modeling (FEM) software.

To further evaluate the potential of MTJ biosensor, we simulate the signal of a submicron-sized MTJ sensor from a *single* NanoTag using a previously published analytical model [9]. Coherent rotation of the free layer under an external magnetic field is assumed in the model. The TMR is calculated from the angle between the magnetization of the free and the pinned layer (θ), which is in turn obtained from the energy minimization equation. The NanoTag used for the simulation is Fe_3O_4 with a diameter of 16 nm and a saturation magnetization of 480 emu/cc. The NanoTag is located at the center of the sensor area, and 30 nm above the sensor surface. The magnetic field from this superparamagnetic particle induced by an external DC bias field (100 Oe) is averaged over the sensor area ($1 \times 0.3\,\mu m^2$). The sensor parameters are taken from the experimental values of typical MTJs (TMR = 50% @ 1 mV bias, $\Delta V_{max} = 150$ mV, $H_k = 40$ Oe, free layer thickness = 20 Å). For the in-plane detection mode shown in Fig. 2a, a transverse field with an amplitude of 110 Oe along the hard axis of the free layer will generate a large peak-to-peak ΔV of 60 μV due to a single Fe_3O_4 NanoTag. This level of output is about ten times larger than a SV sensor with the similar specifications, making single tag detection more feasible.

In conclusion, the magnetic microarray will allow quantitative and very sensitive detection that is more difficult and expensive with current optical techniques, and will ultimately allow single-molecule detection of DNA or protein at a high speed. This represents a potential "killer application" of magnetic nanotechnology in biology whose importance will become clear in the near future.

The authors acknowledge insightful discussions with Drs. R.J. Wilson, D.B. Robinson, and Prof. R.W. Davis at Stanford University, assistance from Dr. M. Sharma at HP Labs, and support from other members of the BioMag IC project at Stanford and IBM. The use of Stanford Nanofabrication Facility and the assistance from J. Conway are also gratefully acknowledged. This work is supported by DARPA through the US Navy Grant no. N000140210807.

References

[1] M. Schena, R.W. Davis, Microarray Biochip Technology, Eaton Publishing, 2000, pp. 1–18.
[2] D.R. Baselt, US Patent 5,981,297, 1999.
[3] D.R. Baselt, G.U. Lee, M. Natesan, et al., Biosens. Bioelectron. 13 (1998) 731.
[4] M.M. Miller, P.E. Sheehan, et al., J. Magn. Magn. Mater. 225 (2001) 138.
[5] M.C. Tondra, US Patent Application 20020060565 (2002).
[6] D.L. Graham, H.A. Ferreira, J. Bernado, et al., J. Appl. Phys. 91 (2002) 7786.
[7] J. Schotter, P.B. Kamp, A. Becker, et al., Biosens. Bioelectron. 19 (2004) 1149.
[8] G. Li, V. Joshi, R.L. White, et al., J. Appl. Phys. 93 (2003) 7557.
[9] G. Li, S.X. Wang, IEEE Trans. Magn. 39 (2003) 3313.
[10] G. Li, S.X. Wang, S. Sun, IEEE Trans. Magn. 40 (2004) 3000.
[11] S. Sun, H. Zeng, D.B. Robinson, et al., J. Am. Chem. Soc. 126 (2004) 273.
[12] G. Li, S.X. Wang, S. Sun, Unpublished results.
[13] R.J.M. van de Veerdonk, et al., Appl. Phys. Lett. 71 (1997) 2839.